On the Inclusion of Time Derivatives of State Variables for Parametric Model Order Reduction for a Beam on a Nonlinear Foundation

David B. Segala
Naval Undersea Warfare Center,
1176 Howell Street,
Newport, RI 02841
e-mail: david.segala@navy.mil

Peiman Naseradinmousavi
Dynamic Systems and Control Laboratory,
Department of Mechanical Engineering,
San Diego State University,
San Diego, CA 92115
e-mails: pnaseradinmousavi@mail.sdsu.edu;
peiman.n.mousavi@gmail.com

The computational burden of parameter exploration of nonlinear dynamical systems can become a costly exercise. A computationally efficient lower dimensional representation of a higher dimensional dynamical system is achieved by developing a reduced order model (ROM). Proper orthogonal decomposition (POD) is usually the preferred method in projection-based nonlinear model reduction. POD seeks to find a set of projection modes that maximize the variance between the full-scale state variables and its reduced representation through a constrained optimization problem. Here, we investigate the benefits of an ROM, both qualitatively and quantitatively, by the inclusion of time derivatives of the state variables. In one formulation, time derivatives are introduced as a constraint in the optimization formulation—smooth orthogonal decomposition (SOD). In another formulation, time derivatives are concatenated with the state variables to increase the size of the state space in the optimization formulation—extended state proper orthogonal decomposition (ESPOD). The three methods (POD, SOD, and ESPOD) are compared using a periodically, periodically forced with measurement noise, and a randomly forced beam on a nonlinear foundation. For both the periodically and randomly forced cases, SOD yields a robust subspace for model reduction that is insensitive to changes in forcing amplitudes and input energy. In addition, SOD offers continual improvement as the size of the dimension of the subspace increases. In the periodically forced case where the ROM is developed with noisy data, ESPOD outperforms both SOD and POD and captures the dynamics of the desired system using a lower dimensional model.
[DOI: 10.1115/1.4035759]

1 Introduction

In design engineering or parameter exploration, one needs to numerically investigate the dynamical system over many combinations of parameters in order to fully understand the dynamics as the system undergoes design changes (initial conditions, system parameters, material properties, etc.). This is a tremendous computational task depending on the model nonlinearities and the scale (number of degrees-of-freedom) of the discretized numerical representation of the dynamical system. One common approach to reduce the computational burden is to develop lower dimensional representations of the higher dimensional full-scale dynamical system. Depending on the scale and the type of nonlinearity, the computational burden of the lower dimensional representation can be reduced by orders of magnitude as compared to the full-scale dynamic model. Typically, the lower dimensional representation is achieved by developing reduced order models (ROMs) of the full-scale dynamic model.

Simulating the full-scale dynamic model at every design configuration to create an ROM at that particular design is very inefficient from a data storage and computational cost perspective. The idea behind parametric ROMs is to develop an ROM that is valid over a set of design configurations. The set projection modes that allow one to transform the high dimensional model to its lower dimensional representation are determined from the full-scale dynamic model at one (or several) design configurations. Then, these projection modes are used to create the ROM at different designs. As a result, the full-scale dynamic model does not have to be simulated at this new design.

One of the most common approaches in projection-based ROMs of nonlinear systems is proper orthogonal decomposition (POD) [1]. POD determines a set of projection modes that maximize the variance between the state variables of the reduced representation and the dynamical system of interest, in the least squares sense [2]. POD has several counterparts in other fields; these include singular value decomposition [3], Karhunen–Loeve decomposition in stochastic process modeling [3–5], principal component analysis in statistical analysis [3,6], and empirical orthogonal decomposition in atmospheric modeling [7]. Liang et al. [3] discussed the connection between POD, singular value decomposition, and Karhunen–Loeve decomposition. In Ref. [2], the Galerkin projection procedure was combined with POD, to generate low dimensional models that have a large phase space. This methodology has led to the development of low-order models in natural and engineered systems across many domains, such as fluid flow [2,8], structural vibrations and chaotic dynamical systems [1,3,9–12], microelectromechanical systems (MEMS) [13], and aeroelastic systems [14,15]. POD has also been applied to mechanical systems that process a significant amount of nonlinearity, such as nonlinear panel flutter with thermal effects [16], acoustostructural coupled systems of elastic multibody systems [17], and coupled flow problems [18].

There are two common approaches to reduce the complexity of the nonlinearity before proceeding with POD. One approach is the

Contributed by the Dynamic Systems Division of ASME for publication in the Journal of Dynamic Systems, Measurement, and Control. Manuscript received October 6, 2016; final manuscript received January 7, 2017; published online May 24, 2017. Assoc. Editor: Dumitru I. Caruntu.

trajectory piecewise-linear (TPWL) approximation [19], which is based on approximating a nonlinear function by a weighted sum of linearized models at selected points along a state trajectory. TPWL has been successfully applied to several nonlinear systems that are found in circuit simulations and shock propagation [20]. The use of TPWL is hindered due to the difficulty finding a piecewise polynomial that is able to approximate general nonlinear forcing. Alternatively, discrete empirical interpolation method (DEIM) constructs a separate subspace for the approximation of the nonlinear term [21,22]. In this approach, a set of interpolation points are selected via a greedy strategy, and then, the interpolation and projection are combined to approximate the nonlinear function in the subspace. For highly nonlinear problems, many DEIM basis vectors may be required to provide an accurate approximation.

The utilization of additional information in the development of projection modes leads to the creation of smooth orthogonal decomposition (SOD). This methodology incorporates the time derivative of the state variables in the optimization formulation as a constraint. The aim of SOD is determine a set of projection modes that maximize the variance between the state variables of the dynamical system of interest and its reduced representation while maximizing smoothness in the least squares sense [23]. The smoothness is introduced as a constraint by requiring the time derivatives of the state variables to be as smooth in time as possible, or to minimize the roughness of the time derivatives. In Ref. [24], SOD was shown to produce comparable results to POD in estimating modal parameters in undamped, lightly damped, and distributed-parameter vibration systems. Rezaee et al. [25] used SOD to derive the modal parameters of a vehicle suspension system. In the biomechanics community, SOD was used to extract smooth trends from multivariate biomechanical data to determine fatigue markers instead of medical techniques that require invasive physiological measurements [26]. SOD was first introduced into the fluids community by Kuehl et al. [27], which extracted a slowly varying Rossby wave in measured ocean currents using SOD when POD was unable to do so.

Very similar to SOD is state-variable modal decomposition (SVMD) [28,29], which also solves a generalized eigenvalue problem of a matrix of state variables and their time derivatives. In its formulation, a nonsymmetric correlation matrix of state variables and approximations of time derivatives is used as a constraint which closely relates to the formulation of SOD. Due to the very similar nature of SOD, the method will not be presented in this paper since the theme of this paper is on the two different ways to incorporate state variables and their time derivatives into the optimization formulation—as a constraint or an extension of the state space. However, SVMD has shown very significant results in the estimation of modal parameters and compared well SOD and POD. SVMD was first introduced to estimate the mode shapes and natural frequencies from a free response of a generally damped linear multi-degrees-of-freedom system by correlations of the state-variable ensembles. SVMD was later applied to an experimental beam for modal parameter estimation of multi-degrees-of-freedom and continuous systems. As of late, this method has not been shown how it performs and compares to conventional model reduction methods in creating ROMs at single operating points or for parametric ROMs.

In Ref. [30], the concept of subspace robustness was presented which determines whether the subspace used for an ROM will be insensitive to perturbations of the system parameters and initial conditions. This concept was further used in Refs. [31] and [32]. The common theme noted earlier is that SOD-based ROM produces more robust and lower dimensional models than POD-based ROM. SOD showed continual improvement as the number of projection modes were increased, whereas POD did not show continual improvement. In these research efforts, the dynamical systems of interest were noise free. The contribution of this work is twofold: (1) extending the state-space by considering the time derivatives of the state variables in the POD formulation which is called extended state POD (ESPOD) and (2) comparing all the three ROM methodologies when measurement noise is added into the system.

The remainder of the paper is as follows: Sec. 2 defines all the three model reduction methodologies of POD, SOD, and ESPOD along with the concept of subspace robustness. In Sec. 3, the methods are applied to a model of an elastic beam on a nonlinear foundation. In Sec. 4, we compare the three model reduction techniques, and we conclude in Sec. 5.

2 Model Order Reduction

2.1 Projection-Based Reduced Order Models. Consider the general form of the nonlinear dynamical system

$$\dot{y} = f(y,t) \tag{1}$$

where $y \in \mathbb{R}^n$ is a dynamic state variable, $f : \mathbb{R}^n \times \mathbb{R} \mapsto \mathbb{R}^n$ is a nonlinear flow, $t \in \mathbb{R}$ is time, and n is usually twice the number of degrees-of-freedom in the system. From the numerical simulation of Eq. (1), the evenly sampled trajectory points can be arranged in a column matrix $Y = [y_1, y_2, \ldots, y_n] \in \mathbb{R}^{m\times n}$ and a matrix of the time derivatives of the evenly sampled trajectory points $\dot{Y} = [\dot{y}_1, \dot{y}_2, \ldots, \dot{y}_n] \in \mathbb{R}^{m\times n}$. Additionally, we concatenate both matrices such that $Y^\star = [y_1, y_2, \ldots, y_n, \dot{y}_1, \dot{y}_2, \ldots, \dot{y}_n] = [Y\ \dot{Y}] \in \mathbb{R}^{m\times 2n}$. We transform the full-scale dynamical system into a new basis by an appropriate coordinate transformation. In this context, the transformation matrix, $P_k = [e_1, e_2, \ldots, e_n]$, is a matrix composed of projection modes, $\{e_i\}_{i=1}^n$, in its columns whereby the projection modes are determined from some appropriate empirical decomposition method (POD, SOD, and ESPOD). Using the coordinate transformation $q = P_k Y \in \mathbb{R}^k$, the corresponding ROM is

$$\dot{q} = P_k^\dagger f(P_k q, t) \tag{2}$$

where $(.)^\dagger$ indicates the pseudoinverse of (.).

2.2 Proper Orthogonal Decomposition. POD finds the sequence of orthonormal projection modes (proper orthogonal modes (POMs)) $\{u_k\}_{k=1}^n$ for which the first k of these functions gives the best possible k-term approximation of Y in the least squares sense. Mathematically, we express this as a constrained optimization problem

$$\max_u \sum_{k=1}^{n} |\langle y_k, u\rangle|^2 \text{ s.t. } ||u|| = 1 \tag{3}$$

where $\langle\cdot,\cdot\rangle$ indicates the inner product. The amount of variance that is captured by each POM is given by its singular value (or proper orthogonal value (POV)), where

$$\sigma_1 = ||Au_1|| \geq \sigma_2 = ||Au_2|| \geq \cdots \geq \sigma_k = ||Au_k|| \tag{4}$$

In practice, the POMs and POVs are determined by the singular value decomposition [33], or SVD, of the matrix Y. Mathematically, this is expressed as

$$Y = U\Sigma V^{\mathrm{T}} \tag{5}$$

where $U = (u_1, u_2, \ldots, u_n) \in \mathbb{R}^{n\times n}$ is an orthogonal matrix composed of left singular vectors, $V = (v_1, v_2, \ldots, v_m) \in \mathbb{R}^{m\times m}$ is an orthogonal matrix of right singular vectors (which in this case are the needed POMs), $\Sigma \in \mathbb{R}^{n\times m}$ is a matrix with all the elements zero except along the diagonal, and $(.)^{\mathrm{T}}$ represents the matrix transpose. The non-negative elements on the diagonal are POVs and are arranged in decreasing order, i.e., $\sigma_1 > \sigma_2, \ldots, \sigma_r >= 0$. Here, $r = \min(n, m)$.

2.3 Smooth Orthogonal Decomposition. SOD incorporates the time derivatives of the state variable as a constraint in the optimization formulation as opposed to the constraint on orthogonally of projection modes as seen in POD. Similarly to POD, in the SOD formulation, one tries to maximize the variance while minimizing the roughness (or equivalently, maximize the smoothness). Now, the constrained optimization problem is written as

$$\max_{\psi} \sum_{k=1}^{n} |\langle y_k, \psi \rangle|^2 \text{ s.t.} \quad \min_{\psi} \sum_{k=1}^{n} |\langle \dot{y}_k, \psi \rangle|^2 \tag{6}$$

where the SOD-based projection modes (smooth orthogonal modes—SOMs) are not constrained to be orthogonal with respect to each other. Following the same procedure as in POD, the SOMs are typically found by solving the generalized singular value decomposition (GSVD) [33] of the matrix pair, Y and $\dot{Y}$

$$Y = UCX^{\mathrm{T}} \quad \dot{Y} = VSX^{\mathrm{T}} \quad C^{\mathrm{T}}C + S^{\mathrm{T}}S = I \tag{7}$$

where $U \in \mathbb{R}^{m\times m}, V \in \mathbb{R}^{n\times n}$, and $X \in \mathbb{R}^{p\times q}$, and $q = \min(m+n, p)$. Matrix $C \in \mathbb{R}^{m\times m}$ and $S \in \mathbb{R}^{m\times m}$ are the non-negative diagonal matrices. The squared values of C are $C^{\mathrm{T}}C = [\alpha_1, \ldots, \alpha_p^2]$ and of S are $S^{\mathrm{T}}S = [\beta_1, \ldots, \beta_p^2]$, such that $S^{\mathrm{T}}S + C^{\mathrm{T}}C = I$. The ratio $\lambda = \alpha/\beta$ gives the generalized singular values (or smooth orthogonal values—SOVs) or the term-by-term division of diag(C^{TC}) and diag(S^{TS}). The generalized singular vectors (or smooth orthogonal modes—SOMs) are given by X.

2.4 Extended State Proper Orthogonal Decomposition. ESPOD incorporates the time derivatives into the ensemble matrix and proceeds with the classical POD formulation. Now, the state space is increased by n. ESPOD finds the sequence of orthonormal projection modes (extended state proper orthogonal modes—ESPOMs) $\{\vartheta_k\}_{k=1}^{n}$ for which the first k of these functions gives the best possible k-term approximation of $Y^{\star}$ in the least squares sense. Mathematically, we still have the same constrained optimization problem as was presented in POD and is depicted below

$$\max_{\vartheta} \sum_{k=1}^{n} |\langle y_k^{\star}, \vartheta \rangle|^2 \text{ s.t } ||\vartheta|| = 1 \tag{8}$$

In practice, the ESPOMs and extended state proper orthogonal values (ESPOVs) are determined by the SVD of the matrix $Y^{\star}$. Mathematically, this is expressed as

$$Y^{\star} = A\Xi\Gamma^{\mathrm{T}} \tag{9}$$

where $A = (a_1, a_2, \ldots, a_n) \in \mathbb{R}^{n\times n}$ is an orthogonal matrix composed of left singular vectors, $\Gamma = (\vartheta_1, \vartheta_2, \ldots, \vartheta_{2m}) \in \mathbb{R}^{2m\times 2m}$ is an orthogonal matrix of right singular vectors (which in this case are the needed ESPOMs), $\Xi \in \mathbb{R}^{n\times 2m}$ is a matrix with all the elements zero except along the diagonal, and $(.)^{\mathrm{T}}$ represents the matrix transpose. The non-negative elements on the diagonal are singular values and are arranged in decreasing order, i.e., $\xi_1 > \xi_2, \ldots, \xi_r >= 0$. Here, $r = \min(n, 2m)$.

2.5 Subspace Robustness. The key idea behind subspace robustness is a quantitative metric that determines whether the subspace will be insensitive to perturbations of the system parameters and initial conditions [30]. If a subspace is insensitive to these perturbations (e.g., off-design configurations), the subspace will provide a faithful ROM of the system of interest. Therefore, a subspace spanned by the projection modes for model order reduction needs to be insensitive to variations in forcing functions, initial conditions, and system parameters. Conventional choices like POMs would be a good choice but they can vary with initial conditions, system parameters, and forcing functions [34]. Therefore, a decomposition identifies a *robust subspace* if all the subspaces estimated from trajectories starting from different initial conditions and/or perturbed system parameters are mutually and a linearly dependent.

Given a set of s trajectories from different simulations with varied design configurations, the idea is to find when the angle between two subspaces is zero. A k-dimensional subspace can be constructed from determining the projection modes, P_i^k, of the ith trajectory. If the angle between two subspaces (P_i^k and P_j^k) is zero, then the subspaces are linearly dependent or parallel. If the angle between two subspaces is $\pi/2$, then the subspaces are linearly independent or orthogonal. If the different subspaces are nearly parallel then the subspace is robust. The set of k-dimensional subspaces $\{P_i^k\}_{i=1}^{s}$ for the model reduction is estimated from a set of s different trajectories which correspond to different parameter configurations, forcing amplitudes, and initial conditions, which are arranged into a matrix $S = [P_1^k, \ldots, P_s^k]$. The k dominant projection modes are spanned by the K-dimensional subspace of the matrix S. The corresponding *subspace robustness* γ_s^k is given by the ratio of the sum of the largest $K+1$ singular values of matrix S over the sum of all the k singular values

$$\gamma_s^k = \left| 1 - \frac{4}{\pi} \arctan \sqrt{\frac{\sum_{i=k+1}^{n} \sigma_i^2}{\sum_{i=1}^{k} \sigma_i^2}} \right| \tag{10}$$

From Eq. (10), it is clear that if all the individual subspace realizations $P_i^k (i = 1, \ldots, s)$ are mutually linearly dependent ($a_{ij}^k = 0, \forall ij$ as well as $\sigma_i = 0$ for $i = k+1, \ldots, n$), then $\gamma_s^k = 1$ (i.e., S has a rank k), and if they are mostly mutually linearly independent ($a_{ij}^k \sim \pi/2, \forall ij, i \neq j$), then $\gamma_s^k \leq 1 - 4\arctan\sqrt{(n-k)/n}/\pi$ (with guaranteed $\gamma_s^k = 1$). Therefore, the subspace identified through some empirical procedure can only be used for model reduction if its subspace robustness γ_s^k is close to unity. Otherwise that subspace may not capture all the needed system dynamics for particular sets of parameters.

3 Numerical Example

From the perspective of finite element theory for discretized mechanical systems, Eq. (1) is normal written as

$$M\ddot{x} + C\dot{x} + Kx = F(\dot{x}, x, t) \tag{11}$$

where $x \in \mathbb{R}^n$ is a dynamic state variable, t is time, M, C, $K \in \mathbb{R}^{nxn}$ are the global mass, damping, and stiffness matrices, respectively, and $F \in \mathbb{R}^n$ describes any nonlinear forcing components. From Eq. (11), the reduced representation is achieved by the coordinate transformation of $x = Pq$, where $q \in \mathbb{R}^k, k \ll n$ is a reduced state variable, and $P = [e_1, e_2, \ldots, e_n]$ is an appropriate set of projection modes obtained through some empirical methods (e.g., POD, SOD, and ESPOD), the corresponding ROM is

$$P^{\mathrm{T}}MP\ddot{q} + P^{\mathrm{T}}CP\dot{q} + P^{\mathrm{T}}KPq = P^{\mathrm{T}}F(P\dot{q}, Pq, t) \tag{12}$$

The dynamical system that is presented here can be considered as a simple system with proportional damping and cubic restoring forces from the springs. The beam, whose schematic representation is depicted in Fig. 1, is discretized into nine Euler Bernoulli

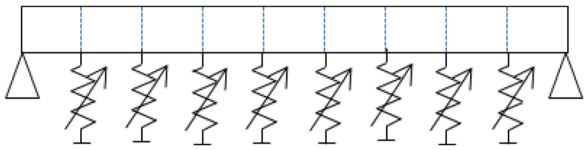

Fig. 1 A simply supported beam on a nonlinear elastic foundation where external forcing is applied at each node and the nonlinear foundation is represented by nonlinear springs at each node

beam elements with two (displacement and rotation) degrees-of-freedom per node. The first and last nodes experience pinned boundary conditions. The steady-state simulation trajectory consisted of 100,000 points with the time-step of 0.007. The equations of motion describing the dynamics of the beam are given by an 18-dimensional second-order equation which is described by Eq. (11), where $\mathbf{M} \in \mathbf{R}^{18\times18}$ is the global mass matrix, $\mathbf{K} \in \mathbf{R}^{18\times18}$ is the global stiffness matrix, $\mathbf{C} \in \mathbf{R}^{18\times18}$ is the global proportional damping matrix, and $F(y, \dot{y}, t)$ can be decomposed into two terms: namely, $f_e(t)$ and $f_n(y)$. The nonlinear foundation is modeled with nonlinear springs, whose nonlinear force is $f_n(y) = y - 2y^3$. The external forcing was equally applied to each node. For periodic forcing, a sine wave $f_e(t) = f \sin \omega t$ with frequency $\omega = 2\pi$ was chosen, and the random forcing was generated by interpolated random sequences.

To generate the data for the subspace robustness, the model was simulated for 21 different forcing amplitudes which were evenly spaced between 0.5 and 10.5. For each new set of forcing amplitudes, ten different initial conditions were used. This resulted in 210 different simulations. For the cases with additive noise, normally distributed noise, $\mathcal{N}(0, 0.5)$, is added to the state variables and the time derivatives of the state variables. It is assumed in these cases that the noise is the same and known. In experimental settings, this will probably not be true, however, the different realizations may be very similar.

4 Results

4.1 Case 1: Periodic Forcing. To quantitatively measure how well our ROM captures the dynamics as the design configurations change, we use subspace robustness (Eq. (10)). Figure 2 depicts the subspace robustness for the 210 different combinations of forcing amplitudes and initial energy for the periodic forcing. For the SOD-based ROM, as the dimension increases the robustness increases monotonically, offering continual improvement after a two-dimensional subspace. There is a slight decrease in robustness from a one- to a two-dimensional subspace. The value reaches unity at a five-dimensional subspace. For both the POD and ESPOD based ROM, the robustness decreases drastically until a nine-dimensional subspace and then increases. In ESPOD, there is an additional decrease in the robustness measure at a 14-dimensional subspace which is not seen in the similar POD-based trend.

Figure 3 qualitatively depicts the results for one particular case. The projection modes are calculated at one design configuration (forcing amplitude in these cases). The projections modes are then used to develop an ROM at a different design configuration (a different forcing amplitude). The projection modes were created with a forcing amplitude of $f = 4.0$, and the ROM was created at a forcing amplitude of $f = 5.5$. The phase portrait of the middle degree-of-freedom of the beam is shown in Fig. 3 (top left) for the full model at a forcing amplitude of $f = 5.5$. The other subplots in the figure represent the three model reduction methods, and their respective titles display the dimension of the ROM. The dimension is determined by minimizing the difference between the power spectral density of the full model and the ROM. The SOD-based ROM is able to produce the dynamics for the system of interest with a lower dimensional model than both POD and ESPOD—both of which require a three-dimensional ROM.

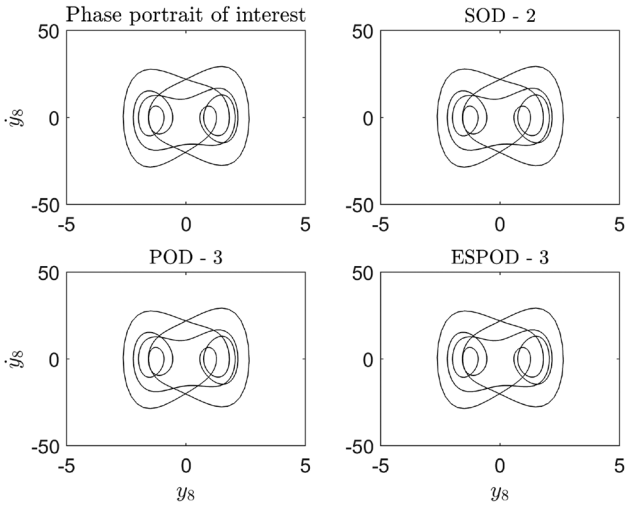

Fig. 3 Phase space portrait for the forcing amplitude $f = 5.5$ (top left) and the resulting SOD, POD, and ESPOD-based phase portrait

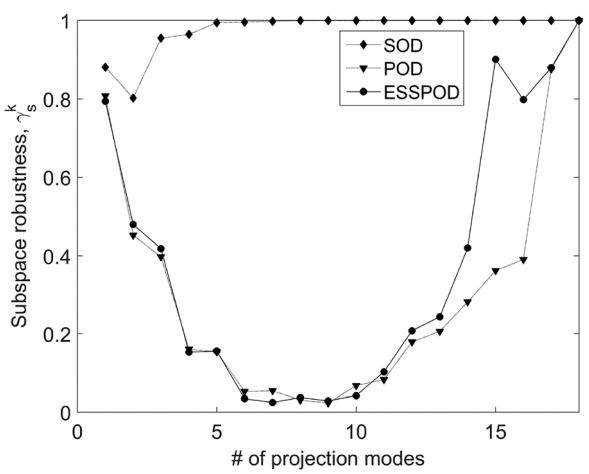

Fig. 2 Subspace robustness for SOD (◇), POD (▽), and ESPOD (○) based ROMs for periodic forcing

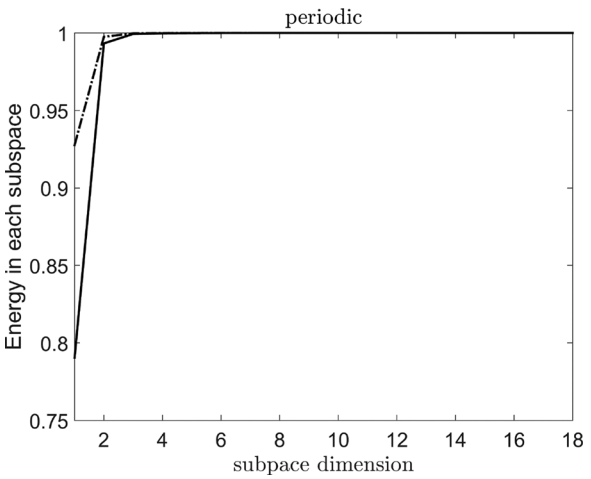

Fig. 4 Energy captured in each subspace for SOD (···), POD (- -), and ESPOD (—)

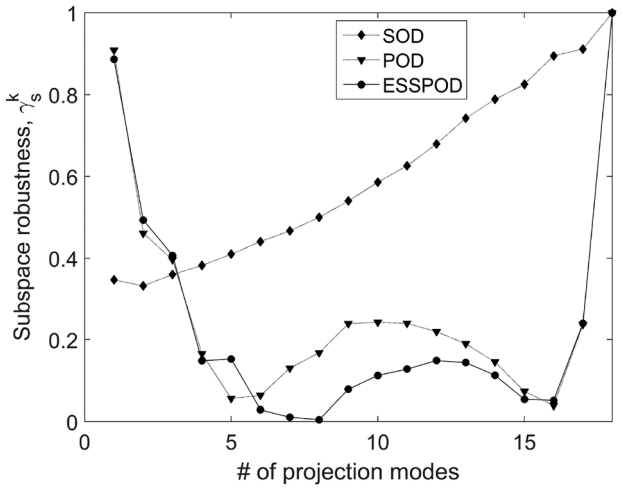

Fig. 5 Subspace robustness for SOD (◇), POD (∇), and ESPOD (◯) based ROMs for periodic forcing with normally distributed noise, $\mathcal{N}(\mathbf{0}, \mathbf{0.5})$

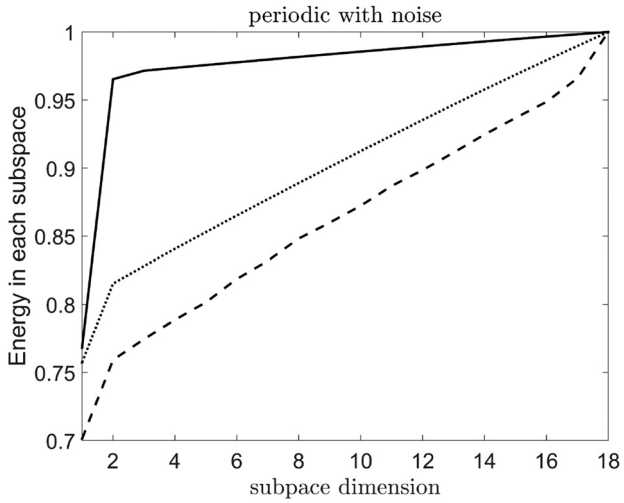

Fig. 7 Energy captured in each subspace for SOD (···), POD (- -), and ESPOD (—)

Finally, the energy in each subspace is depicted in Fig. 4 for SOD (···), POD (- -), and ESPOD (—) based ROMs. Both POD and SOD based ROMs are able to capture more energy in the first two dimensions as compared to ESPOD. However, after a three-dimensional based ROM, all the three methods are comparable.

4.2 Case 2: Periodic Forcing With Noise. For this case, measurement noise, $\mathcal{N}(0, 0.5)$, was added to the state variables and their time derivatives. The projection modes were created with a forcing amplitude of $f = 4.0$, and the ROM was created at a forcing amplitude of $f = 5.5$. There is a significant difference in the SOD and ESPOD based ROM in the subspace robustness as seen in Fig. 5. For the POD-based ROM, the same type of behavior is seen with a decrease of robustness until reaching a certain dimension and then increasing until unity. However, the SOD-based ROM tracks more closely to the POD-based ROM. The ESPOD-based ROM is initially at a very low value; however, it increases monotonically and shows continual over the remaining dimensions and outperforms both POD and SOD.

Figure 6 depicts the individual results for the model at a single forcing amplitude to qualitatively compare how the incorporation of the time derivatives of the state variables affects the performance. With the additive noise in creating the ROM, ESPOD was able to capture the desired dynamics according to the error metric with only a four-dimensional ROM. Likewise, it takes a 17-dimensional SOD-based ROM and a nine-dimensional POD-based ROM to capture the same dynamics.

As depicted in Fig. 7, the energy in each ROM subspace is very similar for the first-dimensional subspace; however, the energy captured in ESPOD-based subspaces greatly increases as the dimension of the subspace increases. Both POD and SOD based ROM continue on the same slope indicating that they increase at a comparative rate.

4.3 Case 3: Random Forcing. Under random forcing, the sensitivity of each ROM method is similar to the periodic forcing case as depicted in Fig. 8. SOD-based ROM offers continual improvement in its ROM and both POD and ESPOD robustness decreases until a nine-dimensional subspace and then increases to the seventh dimension where it reaches a value of unity. Interestingly, unlike the periodic case, SOD does not have an initial decrease in its robustness and ESPOD does not have a decrease at the seventh dimension.

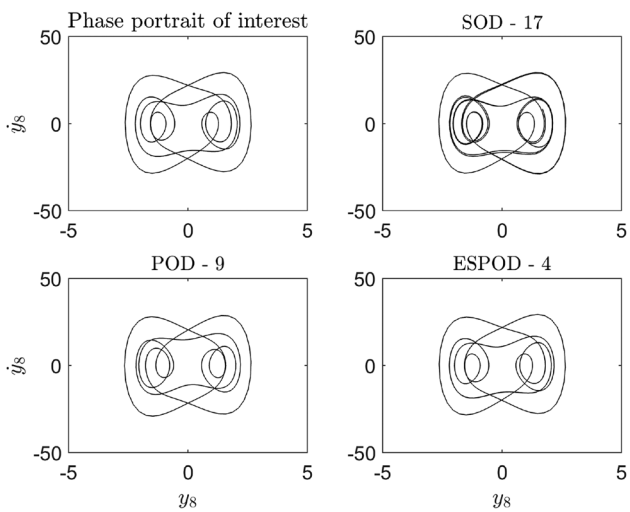

Fig. 6 Phase space portrait for the forcing amplitude $f = 5.5$ (top left) and the resulting SOD, POD, and ESPOD based phase portrait

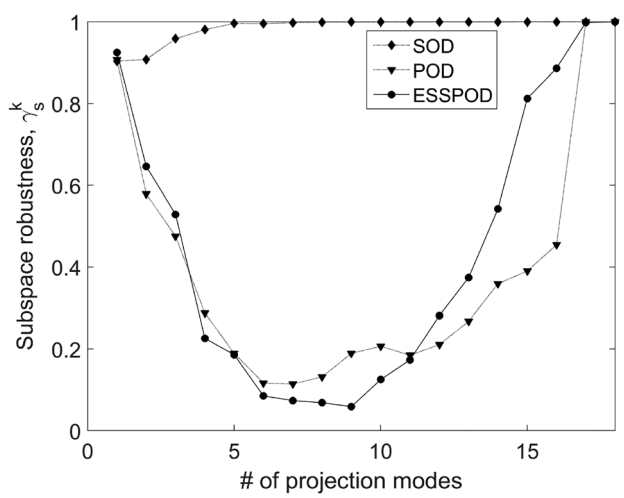

Fig. 8 Subspace robustness for SOD (◇), POD (∇), and ESPOD (◯) based ROMs for random forcing

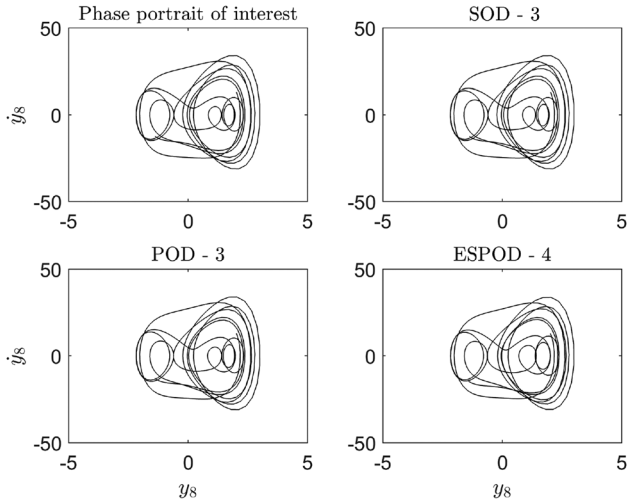

Fig. 9 Phase space portrait for the forcing amplitude $f = 5.5$ (top left) and the resulting SOD, POD, and ESPOD based phase portrait

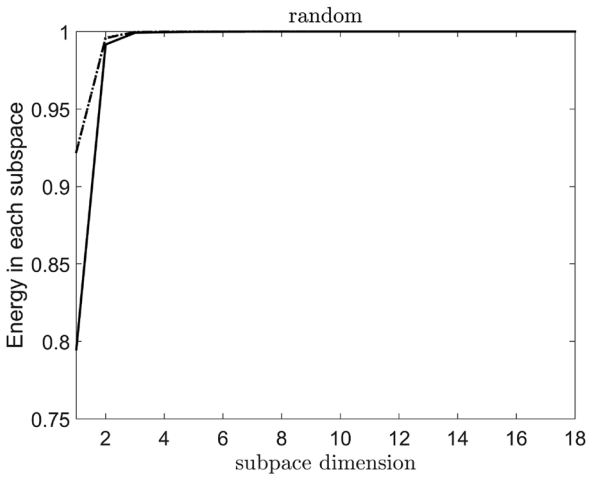

Fig. 10 Energy captured in each subspace for SOD (···), POD (- -), and ESPOD (—)

Similarly, the projection modes were created with a forcing amplitude of $f = 4.0$, and the ROM was created at a forcing amplitude of $f = 5.5$. The qualitative results mimic that of the periodic forcing case as seen in Fig. 9. SOD and POD based ROM are able to capture the dynamics in the lowest dimensional subspace, and ESPOD requires an additional dimension to capture the same dynamics. Finally, the energy in each subspace is depicted in Fig. 10 for SOD (···), POD (- -), and ESPOD (—) based ROMs. Both POD and SOD based ROMs are able to capture more energy in the first two dimensions as compared to ESPOD. However, after a three-dimensional ROM, all the three methods are comparable.

5 Discussion

The purpose of this paper was to compare and contrast the effects of including the time derivative of the state variables into the optimization formulation that is used in the model reduction formulation. In the formulation for SOD, time derivatives were incorporated as a constraint in the optimization formulation. In the formulation of ESPOD, time derivatives are used in conjunction with the state variables and solve the same optimization problem that is formulated for POD. The dynamical system that is used is of a pinned–pinned beam that rests on a nonlinear foundation. The beam is forced both periodically and randomly. For the periodic forcing case, we also consider additive measurement noise in the state variables and their time derivatives. The noise for both the state variables and their time derivatives was the same. Under certain conditions, this may be true in experimental settings, however, under other conditions, the noise will not be the same—maybe similar. The springs that are used to represent the nonlinear foundation are modeled by a nonlinear cubic restoring force. Therefore, it should just be noted that the results drawn from this work cannot be taken on the premise that it will work under every condition. A more formal mathematical framework needs to be completed in order to make that claim.

For parametric ROMs, the goal is to create the ROM for the system under a certain set of parameters and have the ROM be valid if those system parameters change. An ROM that is insensitive to parameter changes, or design configurations, is said to be robust. Utilizing the metric of subspace robustness, the sensitivity to changes in forcing amplitudes and initial conditions (i.e., input energy) is quantitatively assessed. A total of 210 different combinations were used for all the three cases, and it was observed that under periodic and random forcing, SOD-based ROMs create a subspace that is insensitive to parameter changes. As the dimension of the subspace increases, the accuracy of the ROM will continually increase. When measurement noise was included, ESPOD outperformed both SOD and POD based ROMs. In POD and ESPOD, there is a significant decrease in the robustness before it increases. This is seen in the first two cases with SOD in the first dimension. In POD and ESPOD, it is speculated that this is due to orthogonality constraint of the modes. However, SOD does not have this constraint, yet it was still observed—but not as serve. More investigation needs to be carried out to understand the differences in modes between the three methods.

From a qualitative perspective, SOD-based ROMs were able to capture the dynamics using a lower dimensional subspace than both POD and ESPOD for the periodic and random forcing case with no measurement noise. When measurement noise was added into the periodic forcing case, ESPOD significantly outperformed both SOD and POD based ROM. In fact, an SOD-based ROM dimension was almost equal to the dimension of the full-scale model so very little benefit was observed. POD-based ROM was able to capture the dynamics in about half the number of dimensions that SOD needed but still far greater than the number of dimensions that ESPOD needed.

These results compare well with the energy captured in each subspace. Again, for both periodic and randomly forced cases with no measurement noise, SOD and POD were able to capture the same about of energy in its subspace. This aligns well with the phase portrait results that were roughly the same size dimensional ROM, which was needed to capture the dynamics. However, in the periodic forcing case with measurement noise, ESPOD captures significantly more energy in each dimensional subspace than its counterparts of POD and SOD.

The phase portraits add a visual means for understanding the complex dynamics that these methods are able to capture. However, in a realistic scenario they may not be needed. The robustness measure is going to give insight into how well the model reduction approach is suitable for capturing the dynamics at different design configurations. Additionally, this measure can be used to determine the extents of how the model reduction method performs in the parameter space as that parameter space is increased. When the robustness is not close to unity at the full dimension of the model, the calculated projection modes are no longer capturing the nonlinear manifold and the dynamics are being missed. At a single design configuration, the energy in each subspace can be used because it allows one to see how much of the energy is being captured from more than just the phase portraits which can elude someone if there are slight changes that are not easily noticeable.

6 Conclusion

Proper orthogonal decomposition is a projection-based reduced order modeling technique that determines an optimal set of projection modes that maximize the variance between the state variables of the reduced representation and the dynamical system of interest, in the least squares sense. In the optimization formulation, the projection modes are constrained to be orthogonal to each other. Here, we introduce time derivatives of the state variables into the optimization problem for the development of ROMs of parametric dynamical systems. First, the time derivatives are introduced as a constraint in the optimization formulation—SOD. Second, the time derivatives are concatenated with the state variables to increase the size of the state space in the optimization formulation—ESPOD. The three methods (POD, SOD, and ESPOD) are compared and contrasted using a periodically, periodically forced with measurement noise, and a randomly forced beam on a nonlinear foundation. When no measurement noise is included in the data, SOD will give the lowest dimensional ROM to capture the dynamics of the system. When measurement noise is present in the data, ESPOD is the preferred choice and will create the lowest dimensional ROM needed to capture the dynamics.

Acknowledgment

Portions of this work were supported by the Naval Undersea Warfare Center Division Newport Internal Investments.

Nomenclature

u = POMs
Y = matrix of state variables
y_k = kth column of the state-variable matrix Y
$\dot{y}_k$ = time derivative of the kth column of the state-variable matrix Y
$Y^\star$ = matrix of state variables and their time derivatives
γ_s^k = subspace robustness
$y_k^\star$ = kth column of the state and time derivative variable matrix $Y^\star$
λ = SOVs
ξ = ESPOVs
σ = POVs
ψ = SOMs
ϑ = ESPOMs

References

[1] Kerschen, G., Golinval, J.-C., Vakakis, A. F., and Bergman, L. A., 2005, "The Method of Proper Orthogonal Decomposition for Dynamical Characterization and Order Reduction of Mechanical Systems: An Overview," Nonlinear Dyn., **41**(1–3), pp. 147–169.
[2] Holmes, P., Lumley, J. L., and Berkooz, G., 1998, *Turbulence, Coherent Structures, Dynamical Systems and Symmetry*, Cambridge University Press, New York.
[3] Liang, Y. C., Lee, H. P., Lim, S. P., Lin, W. Z., Lee, K. H., and Wu, C. G., 2002, "Proper Orthogonal Decomposition and Its Applications—Part I: Theory," J. Sound Vib., **252**(3), pp. 527–544.
[4] Loeve, M., 1955, *Probability Theory*, D. Van Nostrand Company, Princeton, NJ.
[5] Kosambi, D. D., 1943, "Statistics in Function Space," J. Indian Math. Soc., **7**, pp. 76–88.
[6] Hotelling, H., 1933, "Analysis of a Complex of Statistical Variables Into Principal Components," J. Educ. Psychol., **24**(6), pp. 417–441.
[7] North, G. R., Bell, T. L., Cahalan, R. F., and Moeng, F. J., 1982, "Sampling Errors in the Estimation of Empirical Orthogonal Functions," Mon. Weather Rev., **110**(7), pp. 699–706.
[8] Behzad, F., Helenbrook, B. T., and Ahmadi, G., 2015, "On the Sensitivity and Accuracy of Proper-Orthogonal-Decomposition-Based Reduced Order Models for Burgers Equation," Comput. Fluids, **106**, pp. 19–32.
[9] Feeny, B., 2002, "On the Proper Orthogonal Modes and Normal Modes of a Continuous Vibration System," ASME J. Sound Vib., **124**(1), pp. 157–160.
[10] Feeny, B. F., and Kappagantu, R., 1998, "On the Physical Interpretation of Proper Orthogonal Modes in Vibrations," J. Sound Vib., **211**(4), pp. 607–616.
[11] Chatterjee, A., 2000, "An Introduction to the Proper Orthogonal Decomposition," Current Sci., **78**(7), pp. 808–817.
[12] Kerfriden, P., Gosselet, P., Adhikari, S., and Bordas, S. P.-A., 2011, "Bridging Proper Orthogonal Decomposition Methods and Augmented Newton–Krylov Algorithms: An Adaptive Model Order Reduction for Highly Nonlinear Mechanical Problems," Comput. Methods Appl. Mech. Eng., **200**(5), pp. 850–866.
[13] Hung, E. S., and Senturia, S. D., 1999, "Generating Efficient Dynamical Models for Microelectromechanical Systems From a Few Finite-Element Simulation Runs," J. Microelectromech. Syst., **8**(3), pp. 280–289.
[14] Xie, D., Xu, M., and Dowell, E. H., 2014, "Proper Orthogonal Decomposition Reduced-Order Model for Nonlinear Aeroelastic Oscillations," AIAA J., **52**(2), pp. 229–241.
[15] Xie, D., Xu, M., and Dowell, E. H., 2014, "Projection-Free Proper Orthogonal Decomposition Method for a Cantilever Plate in Supersonic Flow," J. Sound Vib., **333**(23), pp. 6190–6208.
[16] Xie, D., Xu, M., Dai, H., and Dowell, E. H., 2015, "Proper Orthogonal Decomposition Method for Analysis of Nonlinear Panel Flutter With Thermal Effects in Supersonic Flow," J. Sound Vib., **337**, pp. 263–283.
[17] Ihrle, S., Lauxmann, M., Eiber, A., and Eberhard, P., 2013, "Nonlinear Modelling of the Middle Ear as an Elastic Multibody System-Applying Model Order Reduction to Acousto-Structural Coupled Systems," J. Comput. Appl. Math., **246**, pp. 18–26.
[18] Li, X., Chen, X., Hu, B. X., and Navon, I. M., 2013, "Model Reduction of a Coupled Numerical Model Using Proper Orthogonal Decomposition," J. Hydrol., **507**, pp. 227–240.
[19] Rewienski, M. J., 2003, "A Trajectory Piecewise-Linear Approach to Model Order Reduction of Nonlinear Dynamical Systems," Ph.D. thesis, Massachusetts Institute of Technology, Boston, MA.
[20] Rewieński, M., and White, J., 2006, "Model Order Reduction for Nonlinear Dynamical Systems Based on Trajectory Piecewise-Linear Approximations," Linear Algebra Appl., **415**(2), pp. 426–454.
[21] Chaturantabut, S., and Sorensen, D. C., 2010, "Nonlinear Model Reduction Via Discrete Empirical Interpolation," SIAM J. Sci. Comput., **32**(5), pp. 2737–2764.
[22] Henneron, T., and Clenet, S., 2014, "Model Order Reduction of Non-Linear Magnetostatic Problems Based on POD and DEI Methods," IEEE Trans. Mag., **50**(2), pp. 33–36.
[23] Chelidze, D., and Liu, M., 2005, "Dynamical Systems Approach to Fatigue Damage Identification," J. Sound Vib., **281**(3–5), pp. 887–904.
[24] Chelidze, D., and Zhou, W., 2006, "Smooth Orthogonal Decomposition Based Modal Analysis," J. Sound Vib., **292**(3–5), pp. 461–473.
[25] Rezaee, M., Shaterian-Alghalandis, V., and Banan-Nojavani, A., 2013, "Development of the Smooth Orthogonal Decomposition Method to Derive the Modal Parameters of Vehicle Suspension System," J. Sound Vib., **332**(7), pp. 1829–1842.
[26] Segala, D. B., Gates, D. H., Dingwell, J. B., and Chelidze, D., 2011, "Nonlinear Smooth Orthogonal Decomposition of Kinematic Features of Sawing Reconstructs Muscle Fatigue Evolution as Indicated by Electromyography," ASME J. Biomech. Eng., **133**(3), p. 031009.
[27] Kuehl, J., DiMarco, S., Spencer, L., and Guinasso, N., 2014, "Application of the Smooth Orthogonal Decomposition to Oceanographic Data Sets," Geophys. Res. Lett., **41**(11), pp. 3966–3971.
[28] Feeny, B., and Farooq, U., 2008, "A Nonsymmetric State-Variable Decomposition for Modal Analysis," J. Sound Vib., **310**(4–5), pp. 792–800.
[29] Farooq, U., and Feeny, B. F., 2012, "An Experimental Investigation of State-Variable Modal Decomposition for Modal Analysis," ASME J. Vib. Acoust., **134**(2), p. 021017.
[30] Segala, D. B., and Chelidze, D., 2014, "Robust and Dynamically Consistent Model Order Reduction for Nonlinear Dynamic Systems," ASME J. Dyn. Syst. Meas. Control, **137**(2), p. 021011.
[31] Ilbeigi, S., and Chelidze, D., 2016, *Model Order Reduction of Nonlinear Euler-Bernoulli Beam*, Springer International Publishing, Cham, Switzerland, pp. 377–385.
[32] Ilbeigi, S., and Chelidze, D., 2017, *Reduced Order Models for Systems With Disparate Spatial and Temporal Scales*, Springer International Publishing, Cham, Switzerland, pp. 447–455.
[33] Golub, G. H., and Van Loan, C. F., 1996, *Matrix Computations*, Johns Hopkins University Press, Baltimore, MD.
[34] Rathinam, M., and Petzold, L. R., 2003, "A New Look at Proper Orthogonal Decomposition," J. Numer. Anal., **41**(5), pp. 1893–1925.